

Competition between Hydrogen Bonding and Proton Transfer during Specific Anion Recognition by Dihomooxocalix[4]arene Bidentate Ureas

Eduardo Martínez-González,[†] Felipe J. González,[‡] José R. Ascenso,[§] Paula M. Marcos,^{*,||,⊥} and Carlos Frontana^{*,†}

[†]Centro de Investigación y Desarrollo Tecnológico en Electroquímica, Parque Tecnológico Querétaro Sanfandila, 76703 Sanfandila, Pedro Escobedo, Querétaro, Mexico

[‡]Departamento de Química del Centro de Investigación y Estudios Avanzados del I.P.N., Av. Instituto Politécnico Nacional 2508, Apdo. Postal 14-740, C. P. 07360, Mexico City, Mexico

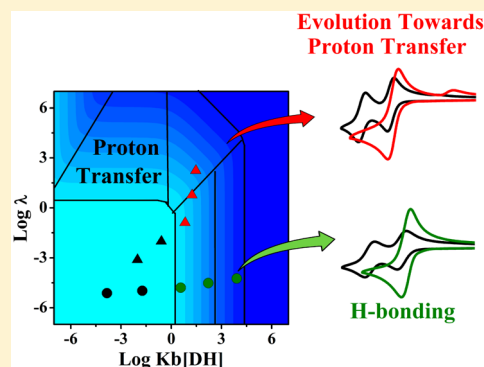
[§]Centro de Química Estrutural, Instituto Superior Técnico, Av. Rovisco Pais, 1049-001 Lisboa, Portugal

^{||}Centro de Química Estrutural, Faculdade de Ciências da Universidade de Lisboa, Edifício C8, 1749-016 Lisboa, Portugal

[⊥]Faculdade de Farmácia da Universidade de Lisboa, Av. Prof. Gama Pinto, 1649-003 Lisboa, Portugal

Supporting Information

ABSTRACT: Competition between hydrogen bonding and proton transfer reactions was studied for systems composed of electrogenerated dianionic species from dinitrobenzene isomers and substituted dihomooxocalix[4]arene bidentate urea derivatives. To analyze this competition, a second-order $E_rC_rC_i$ mechanism was considered where the binding process is succeeded by proton transfer and the voltammetric responses depend on two dimensionless parameters: the first related to hydrogen bonding reactions, and the second one to proton transfer processes. Experimental results indicated that, upon an increase in the concentration of phenyl-substituted dihomooxocalix[4]arene bidentate urea, voltammetric responses evolve from diffusion-controlled waves (where the binding process is at chemical equilibrium) into irreversible kinetic responses associated with proton transfer. In particular, the 1,3-dinitrobenzene isomer showed a higher proton transfer rate constant ($\sim 25 \text{ M}^{-1} \text{ s}^{-1}$) compared to that of the 1,2-dinitrobenzene ($\sim 5 \text{ M}^{-1} \text{ s}^{-1}$), whereas the 1,4-dinitrobenzene did not show any proton transfer effect in the experimental conditions employed.



1. INTRODUCTION

Hydrogen bonding (H-bonding) plays an essential role in a wide range of biological systems and is a basic interaction for designing supramolecular devices with specific applications.¹ This interaction is also important for proton-coupled electron transfer (PCET) reactions which take place in natural and artificial energy transduction processes, including fuel cells, chemical sensors, and cellular respiration.^{2–4} For systems in which electron transfer precedes proton transfer reactions, H-bonding complexes can be present either as intermediates^{5–9} or can determine the energy of transition states.⁹ In both cases, the reaction rate increases due to the appearance of a low-energy barrier pathway,^{8,10} which is dependent on the lifetime of the H-bonded complexes formed. H-bonding complexes can undergo further proton transfer provided that the basicity of the anionic receptor and/or the acidity of the proton donor species are strong enough to abstract or donate the proton, respectively.^{9,11–13}

The competition described above between H-bonding and proton transfer processes has been observed with urea-based

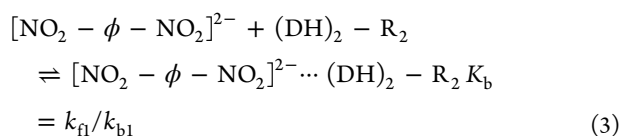
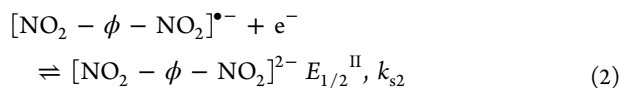
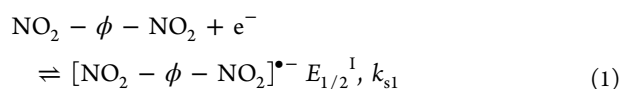
receptors.^{11–16} NH fragments form selective and directional hydrogen bonds with anions, and if they are basic enough and the urea contains strong electron-withdrawing groups, the process evolves toward proton transfer. For example, in a comparative study using *N*-alkyl- and *N*-aryl-(thio)ureas, which act as receptor species for different anions,¹¹ thioureas proved to be more acidic than the respective urea and therefore presented the highest binding constants for H-bonding. Interaction with thioureas evolves into proton transfer when they interact with fluoride anions, and this proton transfer process was enhanced in cases where the urea-based receptor contained electron-withdrawing groups (for example, NO_2).^{11,13} In another work,¹⁶ naphthalenimide moieties were introduced in an urea-based receptor, increasing its acidity and leading to protonate anions with lower basic character, such as H_2PO_4^- and CH_3COO^- . The urea receptor also undergoes a stepwise double deprotonation process in the presence of

Received: April 27, 2016

Published: July 6, 2016

fluoride or hydroxide anions, and this process was dependent on anion concentration. Bergamaschi and collaborators¹⁵ showed also that deprotonation can occur in ureas bearing a positively charged *N*-methylpyridinium residue. However, in this case, proton transfer occurred at the methylene group linking the pyridinium fragment to the receptor skeleton, while the urea moieties of the receptor formed intermolecular hydrogen bonds with the corresponding anions (fluoride and acetate), leading to competition between H-bonding and proton transfer pathways. The anion affinity in these processes can be increased using more preorganized structures of the receptor,¹² for example, calix[*n*]arene skeletons,^{11,17–19} which allows incorporation of more than one urea binding site in its structure and favors its selectivity. This was observed by Jin and collaborators¹⁷ by comparing the binding constants of different anions with calix[4]arene ureas and simple urea and thiourea derivatives. Their results also showed deprotonation of the receptor upon interaction with F⁻, H₂PO₄⁻, and AcO⁻.

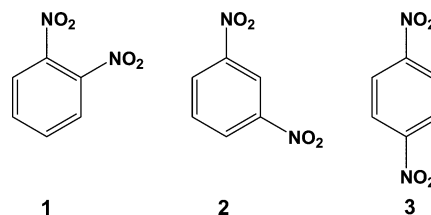
From the above discussion, more information is required about the conditions driving H-bonded systems into proton transfer reactions to fully understand anion recognition processes by these urea derivatives. Also, such a study would complement the growing interest in elucidating H-bonding effects on PCET reactions.^{6–8,10,20–23} Dihomooxalix[4]arene bidentate ureas are interesting H-bond donor species ((HD)₂-R₂) for studying anion recognition, as previous results have shown that they noticeably increase their binding capacity to anions when the nature of the substituent groups in their structures is changed (from *t*-Bu to Ph, *K*_b ranges from ~250 to ~7000 M⁻¹, respectively).^{18,19} Also, by electrogenerating dianions ([NO₂ - φ - NO₂]²⁻) from dinitrobenzene compounds (NO₂ - φ - NO₂), electron transfer-controlled hydrogen bonding (ETCHB) can be studied,^{18,24} leading to increases in the binding affinity when the charge state of the receptor is changed.^{1,18,24,25} ETCHB processes between these latter species can be generally described by the next set of chemical equations:^{18,24}



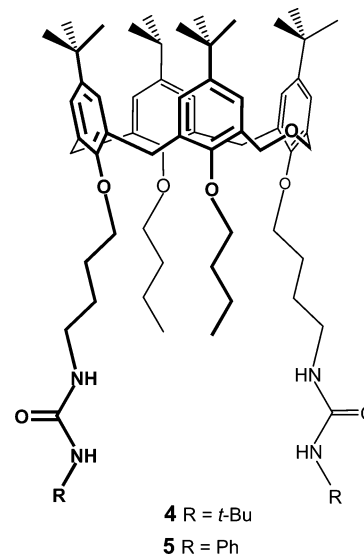
In the process depicted by eq 3, H-bonding occurs between the more basic dinitrobenzene dianions rather than with the electrogenerated anion radical, which is itself not basic enough. As the former species tend to be very basic,²⁴ they could abstract protons from H-bonding donor species, for example, arylureas.²⁴ Therefore, this experimental strategy allows a systematic evaluation of the above-discussed effects between donors and acceptors leading to changes in the overall pathway (either H-bonding and/or proton transfer). By ETCHB, it is also possible to generate unstable anions and dianions, allowing an increase in the variety of studied species other than those proceeding from inorganic or organic salts without the use of chemical reducing agents, which can form ion-pairing species²⁶

and thus prevent the study of H-bonding/proton transfer processes. In this work, ETCHB processes between dinitrobenzene isomers (Scheme 1) and dihomooxalix[4]arene

Scheme 1. Chemical Structures of the Substituted Dinitrobenzene Derivatives Studied



Scheme 2. General Structure of the Dihomooxalix[4]arene Bidentate Ureas Studied ((HD)₂-R₂)



bidentate ureas (Scheme 2) were studied with the aim of identifying molecular properties that modulate binding reactions and proton transfer processes during anion recognition. Results are discussed in terms of the substituent effects on both the receptor and the H-bond donor species and how these substituents determine the kinetic regime for a given donor/acceptor pair.

2. RESULTS AND DISCUSSION

2.1. Competition between H-Bonding and Proton Transfer Reactions. To test the competition process between hydrogen bonding and proton transfer reactions, ETCHB processes were studied using dinitrocompounds (1–3) in their reduced forms as guest species and dihomooxalix[4]arene bidentate ureas bearing *t*-Bu (4) and Ph (5) residues as hosts. Dinitrobenzene isomers undergo two reversible reduction processes in aprotic media to form first a radical anion and then a dianion (Figure 1).²⁴ Addition of urea compound 4 (substituted with *t*-Bu groups), to the solution of dinitrobenzene isomers (1–3) produces little effect on the first voltammetric signal (I_{pc}/I_{pa}), as revealed from the marginal variation of the peak current and potential values (Figures 1A–C). However, the second signal (II_{pa}/II_{pc}) shifts toward less

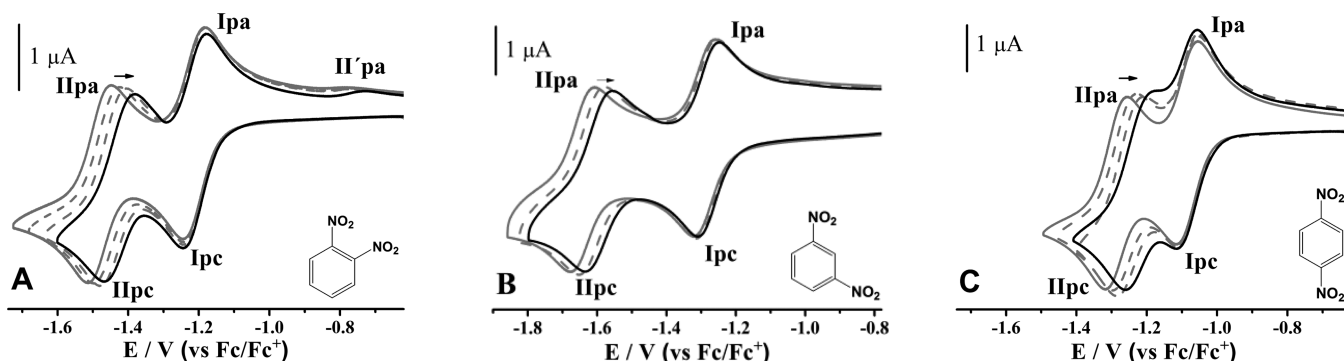


Figure 1. Cyclic voltammograms for 0.0004 mol L⁻¹ 1,2-dinitrobenzene (1, A), 1,3-dinitrobenzene (2, B), and 1,4-dinitrobenzene (3, C) in CH₃CN and 0.1 mol L⁻¹ *n*-Bu₄NPF₆ ($\nu = 0.1$ V s⁻¹, WE: GC (0.0079 cm²)), with different amounts of the urea 4 added. Solid gray lines: [(HD)₂-R₂] = 0 mol L⁻¹. Solid black lines: [(HD)₂-R₂] = 0.0065 mol L⁻¹. Dashed lines show voltammograms obtained with intermediate (HD)₂-R₂ concentrations. Arrows indicate the direction of the shift of the voltammetric signals upon increasing urea concentrations.

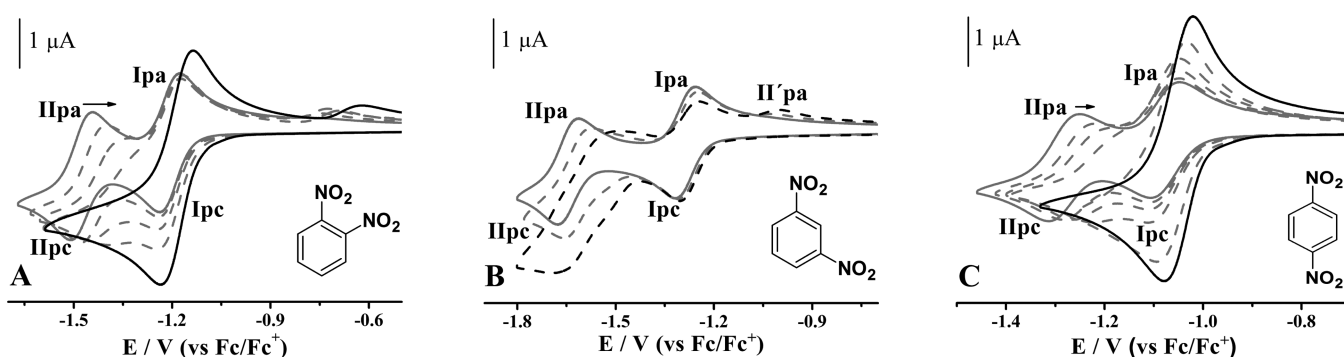


Figure 2. Cyclic voltammograms for 0.0004 mol L⁻¹ 1,2-dinitrobenzene (1, A), 1,3-dinitrobenzene (2, B), and 1,4-dinitrobenzene (3, C) in CH₃CN and 0.1 mol L⁻¹ *n*-Bu₄NPF₆ ($\nu = 0.1$ V s⁻¹, WE: GC (0.0079 cm²)) with different amounts of urea 5 added. Solid gray lines: [(HD)₂-R₂] = 0 mol L⁻¹. Dashed black line: [(HD)₂-R₂] = 0.0006 mol L⁻¹. Solid black lines: [(HD)₂-R₂] = 0.006 mol L⁻¹. Dashed lines show voltammograms obtained with intermediate (HD)₂-R₂ concentrations. Arrows indicate the direction of shifts of the voltammetric signals.

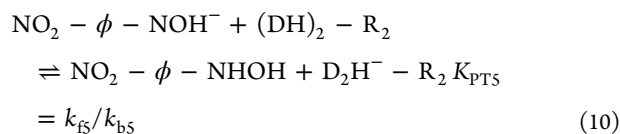
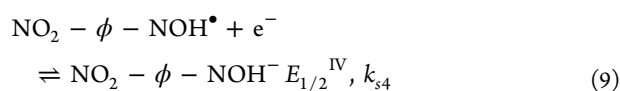
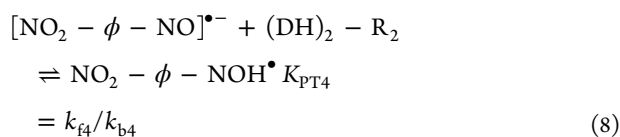
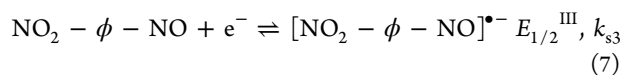
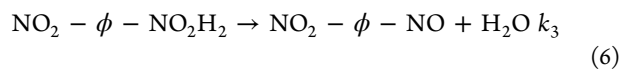
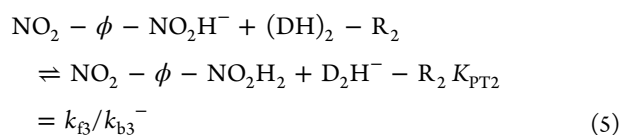
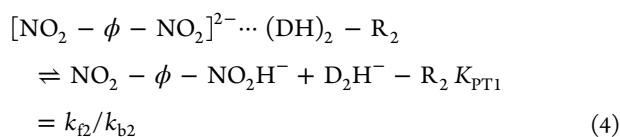
negative potential values upon increasing concentrations of the added urea (Figure 1). This result suggests that the electrogenerated dianions (formed at peak IIc), bind in a fast and reversible reaction with the added urea.²⁴ Due to the presence of the calix[4]arene ring, this interaction could possibly be the formation of inclusion compounds upon interaction between the aromatic ring of the studied dinitrobenzenes and the calix[4]arene moiety, though this process was discarded as the peak current did not decrease (as expected from the change in diffusion coefficients), and the potential shifts would take place in the opposite direction as expected for this reaction.²⁷ Therefore, the experimental results indicate the presence of specific interactions between electrogenerated dianionic species and (HD)₂-R₂ via ETCHB^{1,18,20,24,25} following the mechanism described in eqs 1–3.

The reversible voltammetric behavior observed for both the *meta*- (2) and *para*-dinitrobenzene (3) compounds indicates that the formation of intermolecular H-bonding occurs as a fast and reversible process within the experimental time scale (Figures 1B and C).^{1,18,20,24,25} However, for dinitrobenzene derivative 1, this second reduction step partially loses its reversibility, and upon increasing amounts of urea, a new oxidation peak (II'pa) emerges which is located at more positive potential values than the first reduction step (Figure 1A).

Similar experiments were performed in the presence of the urea compound 5, bearing a phenyl residue, which in turn

increases the acidity of the NH group on the urea moiety.¹⁹ Experimental voltammograms showed more pronounced changes in their shapes (Figure 2), compared with those obtained upon addition of urea 4 (Figure 1). In the case of 3, the second voltammetric signal merges with the first reduction peak upon increasing amounts of added urea, leading to the formation of a two-electron voltammetric wave (Figure 2C).²⁴ For the *ortho*- (1) and *meta*- (2) dinitrobenzene isomers, the second voltammetric signal loses its reversibility (as mentioned above for the interaction between electrogenerated dianions from 1 and urea 4, Figures 2A and B) and also leads to the evolution of voltammetric peak II'pa, in turn related to the formation of a hydroxylamine derivative.^{24,28–30}

The electrochemical behavior described above is consistent with previous experimental results²⁴ where it was proposed that hydroxylamine is the protonated form of the reduced species, uptaking the protons from the host urea compound (NHOH – ϕ – NHOH). In the systems analyzed here, each binding site of the proton donor species (urea derivatives 4 and 5) could protonate each nitro function of the receptor species (compounds 1–3). To simplify the analysis, it was assumed that both the overall mechanism and the respective thermodynamic and kinetic parameters are identical for both NO₂ groups. Therefore, the reactions taking place at any binding site (after the formation of the H-bonding adduct) can be described as follows:



The observed voltammetric behavior (Figures 1 and 2) proved to be dependent on both the relative position of the nitro groups in compounds 1–3 and also on the nature of the substituents present in the studied dihomooxalix[4]arene urea derivatives 4 and 5. In particular, addition of urea 5 to solutions containing dinitrobenzene isomers being reduced (1–3) produced potential shifts larger than those in experiments performed in the presence of urea 4 and also induced the largest changes in the voltammetric responses. These results suggest that there is an enhanced interaction (K_b in eq 3) of the host–guest system with a mutually increased rate of proton transfer (k_{p2} in eq 4) in systems involving the urea residue bearing phenyl substituents. These effects are in accordance with the changes in electrophilicity of the reactive species, specifically with the local electroaccepting power ($\sum_k \omega_k^+(r)$) in the vicinity of the urea region for compounds 4 and 5.¹⁸ For these systems, electronic structure calculations showed $\sum_k \omega_k^+(r)$ values for compound 5 (-3.298×10^{-1}) higher than those for compound 4 (-3.95×10^{-2}).¹⁸ However, experimental results also show that these thermodynamically enhanced recognition effects are accompanied by changes in the reaction mechanism, and therefore, a kinetic strategy is required to discriminate and evaluate the relative binding constant and proton transfer rate from the experimental responses.

2.2. Proton Transfer Kinetic Effects in Voltammetric Responses Involving ETCHB. To rationalize how molecular properties determine proton transfer processes and binding reactions during ETCHB, in the second reduction step of the studied dinitrobenzenes (eqs 1–10), some considerations were taken into account. For instance, only a single one-electron transfer reaction is coupled sequentially with a one-proton transfer process (eqs 2 and 3). The binding reaction should

occur as a fast and reversible process for which the relative rates of both formation and dissociation reactions (k_{f1} and k_{b1}) of the adduct (eq 3) should be very large, as the system is in equilibrium during the binding process.^{20,31,32} For this purpose, both rate constants were fixed at values close to the diffusion limit rate constant for a bimolecular reaction (10^8 s^{-1}).²⁰ Classically, the presence of the binding reaction leads to a shift in the corresponding reduction potentials toward less negative values, exhibiting diffusion-controlled voltammetric waves.^{1,18,24,25} This case can be identified as a DE process.³³

The proton transfer reaction (eq 4) requires the formation of the H-bonded complex ($[\text{NO}_2 - \phi - \text{NO}_2]^{2-} \cdots (\text{DH})_2 - \text{R}_2$), and the transfer rate of this species (k_{p2}) becomes determining in the overall kinetics of the process. Even though this rate is not explicitly dependent on the $(\text{DH})_2 - \text{R}_2$ concentration, such a relationship can be found using the equilibrium constant K_b (eq 3) as follows:

$$\begin{aligned}
 \nu_2 &= k_{\text{p2}}[[\text{NO}_2 - \phi - \text{NO}_2]^{2-} \cdots (\text{DH})_2 - \text{R}_2] \\
 &= k_{\text{p2}}K_b[[\text{NO}_2 - \phi - \text{NO}_2]^{2-}][(\text{DH})_2 - \text{R}_2] \quad (11)
 \end{aligned}$$

Therefore, the reaction becomes a second-order process and also depends on the $(\text{DH})_2 - \text{R}_2$ concentration, as occurring in the binding process (eq 11). This analysis implies that both effects should be considered systematically without underlying the interdependence between them, a consideration which is not usually employed.³³ In this way, the theoretical description of the voltammetric behavior can be described by simulation of the electrochemical processes depicted in eqs 2–4, considering that eq 1 is insensitive to hydrogen bonding effects, and eqs 5–10 are fast enough to not be determining of the overall mechanism. Using voltammetric simulations of the codependent variables (see the Supporting Information), a kinetic zone diagram was constructed to identify the kinetic regimes defining different sets of values between a dimensionless binding parameter (represented as $K_b[(\text{DH})_2 - \text{R}_2]$) and the second-order dimensionless kinetic parameter λ ($\lambda = K_b k_{\text{p2}}[(\text{DH})_2 - \text{R}_2]/\text{RT}/(\nu F)$).^{20,31,33,34} To avoid an intrinsic dependence on the rate of electron transfer, the reduction step (eq 1) was considered to occur quickly ($k_{\text{s1}} = 10000 \text{ cm s}^{-1}$) within the time scale selected for the simulation ($\nu = 1 \text{ V s}^{-1}$).

Different regions define the kinetic diagram obtained (Figure 3), whose characteristics are described in Table 1. These kinetic regions were identified based on specific values expected of both dimensionless peak potential (ξ_{pc}) and current function ($\pi^{1/2}\chi(\sigma t)$) of the voltammetric responses.^{33–35} In general, voltammograms obtained at DO and DE zones show a reversible behavior, while total chemical irreversibility corresponds to KP region. Partial reversibility (with the proton transfer reaction becoming rate determining) occurs at the intermediate zones KE, KG, KG_2 and KG_3 (controlled by the kinetics of proton transfer).

With this zone diagram, it is possible to rationalize the experimental results involved. Upon increasing the urea concentration, ETCHB systems encompass transitions between DO and DE zones where both cathodic and anodic peaks II are shifted toward less negative values without a significant loss of reversibility. From the latter, K_b values can be obtained (e.g., by nonlinear regressions between Epc vs $\log [(\text{DH})_2 - \text{R}_2]$ Figure 4).^{1,18,20} In the case of the systems studied, interactions between urea 4 and dinitrobenzene isomers 2 and 3 would be classified in this zone in addition to the experimental results for the interaction between urea 5 and 3 (Figure 2C).

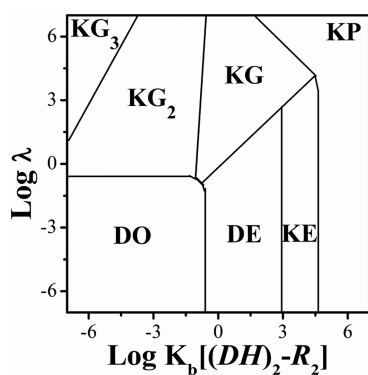


Figure 3. Kinetic zone diagram for variations of the peak potential E_{pc} in a stepwise electron transfer reaction coupled with a proton transfer process involving H-bonding intermediates as a function of both the binding parameter $K_b[(DH)_2 - R_2]$ and the proton transfer kinetic parameter $\lambda = K_b k_{p2} [(DH)_2 - R_2] RT / (\nu F)$ ($k_{s1} = 10000 \text{ cm s}^{-1}$; $\nu = 1 \text{ V s}^{-1}$; $[(DH)_2 - R_2] = 1 \text{ mol L}^{-1}$).

For systems involving proton transfer effects, only the regions where an explicit dependence on the $[(DH)_2 - R_2]$ concentration are of use, as shown by the experimental results. This behavior occurs at the KG zone, which is intermediate between the transitions from pure diffusion control to pure kinetic conditions. Under these circumstances, experimental E_{pc}^{II} values together with the simulated working curves can be used to analyze both binding and kinetic effects (Figure 5). The working curves were taken in a wide range of λ values along the variation of the parameter $K_b[(DH)_2 - R_2]$. From this analysis, experimental values of both K_b and k_{p2} are shown in Table 2. It

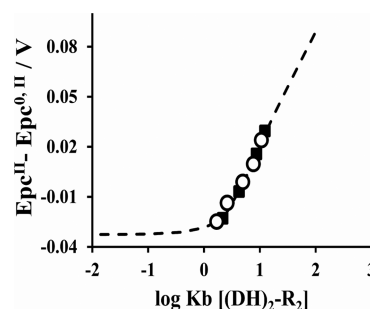


Figure 4. Experimental variations of the peak potential E_{pc} for 1,4-dinitrobenzene as a function of the parameter $K_b[(DH)_2 - R_2]$ for different concentrations of the dihomooxalix[4]arene urea substituted with (■) Ph and (○) *t*-Bu groups.

should be noticed that only k_{p2} was determined, as the remaining protonation steps are not typically rate determining.^{28–30} and were not considered in the mechanism used for simulation.

From the analysis performed, phenyl urea 5 is a stronger receptor than *tert*-butyl urea 4 and also leads to proton transfer effects upon interaction with dinitrobenzene anionic species electrogenerated from compounds 1 and 2 due to the higher acidity of their NH groups.¹⁹ Both urea compounds show in general higher K_b values for the interaction with the studied dianion species compared to previous results with the single anion radical species,¹⁸ which is consistent with previously obtained data showing that this kind of electrogenerated dianions are stronger H-bond acceptors.²⁴ On the other hand, data in Table 2 also indicate a clear preference of ureas 4 and 5,

Table 1. Voltammetric Peak Properties of the Responses Obtained as a Function of $[(DH)_2 - R_2]$ and ν at a Constant Temperature of 298.15 K

kinetic zone	voltammetric peak properties	
	dimensionless peak potential (ξ_{pc})	dimensionless peak current ($\pi^{1/2}\chi(\sigma t)$)
DO	$\xi_{pc} \neq f(\log[(DH)_2 - R_2]) \neq f(\log \nu)$ $\xi_{pc} \neq f(\log \nu) = f(\log[(DH)_2 - R_2])$	$\pi^{1/2}\chi(\sigma t) = 0.4463$
DE	$\frac{dE_p}{d(\log[(DH)_2 - R_2])} = 60 \text{ mV dec}^{-1}$ $\xi_{pc} \neq f(\log \nu) = f(\log[(DH)_2 - R_2])$	$\pi^{1/2}\chi(\sigma t) = 0.4463$
KE	$60 > \frac{dE_p}{d(\log[(DH)_2 - R_2])} = 0 \text{ mV dec}^{-1}$	$0.4958 > \pi^{1/2}\chi(\sigma t) > 0.4463$
KP	$\xi_{pc} \neq f(\log[(DH)_2 - R_2]) \neq f(\log \nu)$ $\xi_{pc} = f(\log[(DH)_2 - R_2]) = f(\log \nu)$	$\pi^{1/2}\chi(\sigma t) = 0.4958$
KG	$60 > \frac{dE_p}{d(\log[(DH)_2 - R_2])} = 0 \text{ mV dec}^{-1}$ $30 > \frac{dE_p}{d(\log \nu)} > 0 \text{ mV dec}^{-1}$ $\xi_{pc} \neq f(\log[(DH)_2 - R_2]) = f(\log \nu)$	$0.4958 > \pi^{1/2}\chi(\sigma t) > 0.4463$
KG ₂	$\frac{dE_p}{d(\log \nu)} > 0 \text{ mV dec}^{-1}$ $\xi_{pc} \neq f(\log \nu) = f(\log[(DH)_2 - R_2])$	$0.4958 > \pi^{1/2}\chi(\sigma t) > 0.4463$
KG ₃	$\frac{dE_p}{d(\log[(DH)_2 - R_2])} = 60 \text{ mV dec}^{-1}$	$0.4463 > \pi^{1/2}\chi(\sigma t) > 0.38$

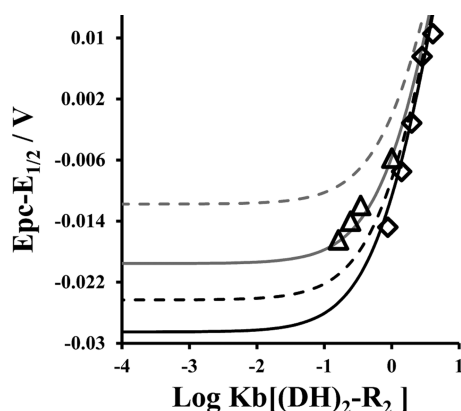


Figure 5. Experimental variations of the peak potential E_{pc} for 1,2-dinitrobenzene (\diamond) and 1,3-dinitrobenzene (Δ) as a function of the kinetic parameter $K_b[(DH)]$ for different concentrations of the dihomooxalix[4]arene urea bearing Ph groups. Lines represent simulated variations for different values: black line, $\log \lambda = -7$; black dashed line, $\log \lambda = -0.6$; gray line, $\log \lambda \sim 0$; and gray dashed line, $\log \lambda = 0.6$.

Table 2. Kinetic and Thermodynamic Data Obtained upon Fitting Experimental E_{pc}^{II} Values with Those Obtained with Simulated ETCHB

dinitro compound	<i>t</i> -Bu urea (4)		Ph urea (5)	
	K_b ($\times 10^{-2} M^{-1}$)	k_{t2} ($M^{-1} s^{-1}$)	K_b ($\times 10^{-2} M^{-1}$)	k_{t2} ($M^{-1} s^{-1}$)
1	12	below experimental error	103	~ 5
2	13	N.A. ^a	18	~ 25
3	17	N.A. ^a	220	N.A. ^a

^aN.A.: not acquired.

depending on the dinitrobenzene substitution pattern. As observed in another study with 1,3-diphenylurea,²⁴ 1,3-dinitrobenzene is prone to be protonated with phenyl-substituted ureas. In this *meta* isomer, a direct resonance between the two nitro groups is not possible, resulting in less delocalization of the negative charge and consequently stronger H-bonding by the NH residues of the urea compound. However, this effect also provokes an increase in the protonation rate (Table 2), thus decreasing the stability of the H-bonded adduct. The slight preference for the 1,4-dinitrobenzene *para* isomer in the case of *tert*-butyl urea 4 should be related to steric hindrance caused by the *tert*-butyl groups. On the other hand, kinetic results suggest that binding reactions between urea compound 5 and isomers 2 and 3 are quickly affected by slow proton transfer reactions, as was observed experimentally, because small values of k_{t2} (~ 5) cause an important loss in experimental reversibility (Figure 2B). These results suggest that further increases in k_{t2} could be obtained by adding electron-withdrawing groups (e.g., CF_3 , NO_2) to the phenyl urea substituent, thus increasing the acidity of the NH protons. Preparation of these molecules could provide interesting transitions to study behavior in the kinetic regions KG_2 , KG_3 , and KP , which were not observed in this work.

3. CONCLUSIONS

Experimental evidence for competition between hydrogen bonding and proton transfer reactions was obtained for systems composed of electrogenerated dianionic species from dinitrobenzene isomers and substituted dihomooxalix[4]arene bidentate urea derivatives. To analyze this competition, a second-order $E_rC_rC_i$ mechanism was considered where the binding process is succeeded by proton transfer, and the voltammetric responses become a function of two dimensionless parameters: the first related to binding reactions ($K_b[(DH)]$) and the second related to the proton transfer process ($\lambda = K_b k_{t2} [(DH)] RT / (\nu F)$). Experimental results indicate that, upon an increase in phenyl-substituted dihomooxalix[4]arene bidentate urea, voltammetric responses evolve from diffusion-controlled waves (where the binding process is at chemical equilibrium) into kinetic irreversible responses associated with proton transfer. In particular, 1,3-dinitrobenzene showed a higher proton transfer rate constant ($k_{t2} \sim 25 M^{-1} s^{-1}$) compared to that of 1,2-dinitrobenzene ($k_{t2} \sim 5 M^{-1} s^{-1}$), whereas 1,4-dinitrobenzene did not show any proton transfer effect in the experimental conditions employed.

4. EXPERIMENTAL SECTION

4.1. Chemicals and Reagents. Electrochemical experiments were carried out using 0.0004 mol L^{-1} solutions of 1,2-(1), 1,3-(2) and 1,4-dinitrobenzene (3) isomers (Scheme 1), AR grade without further purification, dissolved in acetonitrile (dried over molecular sieve) and containing 0.1 mol L^{-1} tetrabutylammonium hexafluorophosphate (*n*-Bu₄NPF₆, dried at 105 °C overnight before use) as supporting electrolyte. All solutions were maintained under an inert atmosphere by saturation with high-purity nitrogen (grade 5.0) at room temperature (approximately 20 °C). These experiments were also performed in the presence of increasing amounts of 0.007 mol L^{-1} solutions of a series of dihomooxalix[4]arene bidentate urea derivatives substituted with *t*-Bu (4) and Ph (5) residues which were synthesized following a previously reported procedure (Scheme 2).¹⁹ The titration solutions of the ureas contained 0.1 mol L^{-1} *n*-Bu₄NPF₆/CH₃CN and 0.0004 mol L^{-1} of the corresponding dinitrobenzene isomer to avoid dilution.

4.2. Instrumentation. Electrochemical experiments were performed using a potentiostat at a scan rate of $\nu = 0.1 V s^{-1}$, applying IR drop compensation with Ru values determined from positive feedback measurements ($R_u \sim 600 \Omega$).^{36,37} A glassy carbon disk electrode (0.0079 cm²) was used as the working electrode. The surface was polished with 0.05 μm diamond powder and rinsed successively with acetone and acetonitrile before each voltammetric run. A platinum wire served as the auxiliary electrode, using as the reference electrode a nonaqueous commercial electrode Ag/0.01 mol L^{-1} AgNO₃ + 0.1 mol L^{-1} *n*-Bu₄NClO₄ in acetonitrile. The potential of the silver reference electrode was measured versus the redox potential of the ferrocene/ferrocenium (Fc/Fc⁺) couple under the same conditions of the other experiments as recommended by IUPAC.³⁸ Voltammetric simulations were performed using the software BAS-DigiSim 3.03b.

■ ASSOCIATED CONTENT

Supporting Information

The Supporting Information is available free of charge on the ACS Publications website at DOI: 10.1021/acs.joc.6b00962.

Simulated working curves for dimensionless peak potential and current as a function of the dimensionless parameters $K_b[(DH)_2 - R_2]$ and $\lambda = K_b k_{t2} [(DH)_2 - R_2] RT / (\nu F)$. (PDF)

■ AUTHOR INFORMATION

Corresponding Authors

*E-mail: pmmarcos@fc.ul.pt, Tel.: +351 217500111, Fax: +351 21 7500979.

*E-mail: cfrontana@cideteq.mx, Tel.: +52 442 2116000 Ext. 7849, Fax.: +52 442 2116001.

Notes

The authors declare no competing financial interest.

■ ACKNOWLEDGMENTS

E.M.-G. thanks CONACyT-Mexico for economical support of the graduate studies. C.F. thanks Conacyt for financial support through Project 207688 (Joint Project between Conacyt-Mexico and BMF).

■ REFERENCES

- (1) Martínez-González, E.; Frontana, C. *J. Org. Chem.* **2014**, *79*, 1131–1137.
- (2) Hammes-Schiffer, S.; Stuchebrukhov, A. A. *Chem. Rev.* **2010**, *110*, 6939–6960.
- (3) Costentin, C.; Robert, M.; Savéant, J. M. *Chem. Rev.* **2010**, *110*, PR1–PR40.
- (4) Trumpower, B. L.; Gennis, R. B. *Annu. Rev. Biochem.* **1994**, *63*, 675–716.
- (5) Arunan, E.; Desiraju, G. R.; Klein, R. A.; Sadlej, J.; Scheiner, S.; Alkorta, I.; Clary, D. C.; Crabtree, R. H.; Dannenberg, J. J.; Hobza, P.; Kjaergaard, H. G.; Legon, A. C.; Mennucci, B.; Nesbitt, D. J. *Pure Appl. Chem.* **2011**, *83*, 1637–1641.
- (6) Mader, E. A.; Mayer, J. M. *Inorg. Chem.* **2010**, *49*, 3685–3687.
- (7) Alligrant, T. M.; Alvarez, J. C. *J. Phys. Chem. C* **2011**, *115*, 10797–10805.
- (8) Clare, L. A.; Pham, A. T.; Magdaleno, F.; Acosta, J.; Woods, J. E.; Cooksy, A. L.; Smith, D. K. *J. Am. Chem. Soc.* **2013**, *135*, 18930–18941.
- (9) Epshtein, L. M. *Russ. Chem. Rev.* **1979**, *48*, 854–867.
- (10) Staley, P. A.; Lopez, E. M.; Clare, L. A.; Smith, D. K. *J. Phys. Chem. C* **2015**, *119*, 20319–20327.
- (11) Li, A.-F.; Wang, J.-H.; Wang, F.; Jiang, Y.-B. *Chem. Soc. Rev.* **2010**, *39*, 3729–3745.
- (12) Baggi, G.; Boiocchi, M.; Fabbrizzi, L.; Mosca, L. *Chem. - Eur. J.* **2011**, *17*, 9423–9439.
- (13) Amendola, V.; Esteban-Gómez, D.; Fabbrizzi, L.; Licchelli, M. *Acc. Chem. Res.* **2006**, *39*, 343–353.
- (14) Boiocchi, M.; Del Boca, L.; Gómez, D. E.; Fabbrizzi, L.; Licchelli, M.; Monzani, E. *J. Am. Chem. Soc.* **2004**, *126*, 16507–16514.
- (15) Bergamaschi, G.; Boiocchi, M.; Monzani, E.; Amendola, V. *Org. Biomol. Chem.* **2011**, *9*, 8276.
- (16) Esteban-Gómez, D.; Fabbrizzi, L.; Licchelli, M. *J. Org. Chem.* **2005**, *70*, 5717–5720.
- (17) Jin, C.; Zhang, M.; Deng, C.; Guan, Y.; Gong, J.; Zhu, D.; Pan, Y.; Jiang, J.; Wang, L. *Tetrahedron Lett.* **2013**, *54*, 796–801.
- (18) Martínez-González, E.; Armendáriz-Vidales, G.; Ascenso, J. R.; Marcos, P. M.; Frontana, C. *J. Org. Chem.* **2015**, *80*, 4581–4589.
- (19) Marcos, P. M.; Teixeira, F. A.; Segurado, M. A. P.; Ascenso, J. R.; Bernardino, R. F.; Michel, S.; Hubscher-Bruder, V. *J. Org. Chem.* **2014**, *79*, 742–751.
- (20) Martínez-González, E.; Frontana, C. *Phys. Chem. Chem. Phys.* **2014**, *16*, 8044–8050.
- (21) Belkova, N. V.; Collange, E.; Dub, P.; Epstein, L. M.; Lemenovskii, D. A.; Lledós, A.; Maresca, O.; Maseras, F.; Poli, R.; Revin, P. O.; Shubina, E. S.; Vorontsov, E. V. *Chem. - Eur. J.* **2005**, *11*, 873–888.
- (22) Tamashiro, B. T.; Cedano, M. R.; Pham, A. T.; Smith, D. K. *J. Phys. Chem. C* **2015**, *119*, 12865–12874.
- (23) Ishikita, H.; Saito, K. *J. R. Soc., Interface* **2014**, *11*, 20130518.
- (24) Chan-Leonor, C.; Martin, S. L.; Smith, D. K. *J. Org. Chem.* **2005**, *70*, 10817–10822.
- (25) Bu, J.; Lilienthal, N. D.; Woods, J. E.; Nohrden, C. E.; Hoang, K. T.; Truong, D.; Smith, D. K. *J. Am. Chem. Soc.* **2005**, *127*, 6423–6429.
- (26) Echegoyen, L.; Hidalgo, H.; Stevenson, G. R. *J. Phys. Chem.* **1973**, *77*, 2339–2342 and 2649–2652.
- (27) Kaifer, A. E. In *Electrochemistry of Functional Supramolecular Systems*; John Wiley & Sons, Inc.: New York, 2009; pp 59–85.
- (28) Morales-Morales, J. A.; Frontana, C.; Aguilar-Martínez, M.; Bautista-Martínez, J. A.; González, F. J.; González, I. *J. Phys. Chem. A* **2007**, *111*, 8993–9002.
- (29) Pérez-Jiménez, A. I.; Frontana, C. *Electrochim. Acta* **2012**, *82*, 463–469.
- (30) Amatore, C.; Capobianco, G.; Farnia, G.; Sandoná, G.; Saveant, J. M.; Severin, M. G.; Vianello, E. *J. Am. Chem. Soc.* **1985**, *107*, 1815.
- (31) Savéant, J. M. *J. Phys. Chem. B* **2001**, *105*, 8995–9001.
- (32) Savéant, J. M. *J. Am. Chem. Soc.* **2008**, *130*, 4732–4741.
- (33) Mastragostino, M.; Nadjo, L.; Savéant, J. M. *Electrochim. Acta* **1968**, *13*, 721–749.
- (34) Bard, A.; Faulkner, L. *Electrochemical Methods, Fundamentals and Applications*, 2nd ed.; John Wiley and Sons: New York, 2001.
- (35) Nicholson, R. S.; Shain, I. *Anal. Chem.* **1964**, *36*, 706.
- (36) Roe, D. K. In *Laboratory Techniques in Electroanalytical Chemistry*, 2nd ed.; Kissinger, P., Heineman, W. R., Eds.; Taylor & Francis: Abingdon, Oxon, U.K., 1996.
- (37) He, P.; Faulkner, L. R. *Anal. Chem.* **1986**, *58*, 517–523.
- (38) Gritzner, G.; Kuta, J. *Pure Appl. Chem.* **1984**, *56*, 461–466.